RESEARCH ARTICLE

TGF-β family ligands exhibit distinct signalling dynamics that are driven by receptor localisation

Daniel S. J. Miller[1,*], Bernhard Schmierer[2] and Caroline S. Hill[1,‡]

ABSTRACT

Growth factor-induced signal transduction pathways are tightly regulated at multiple points intracellularly, but how cells monitor levels of extracellular ligand and translate this information into appropriate downstream responses remains unclear. Understanding signalling dynamics is thus a key challenge in determining how cells respond to external cues. Here, we demonstrate that different TGF-β family ligands, namely activin A and BMP4, signal with distinct dynamics, which differ profoundly from those of TGF-β itself. The signalling dynamics are driven by differences in the localisation and internalisation of receptors for each ligand, which in turn determine the capability of cells to monitor levels of extracellular ligand. By using mathematical modelling, we demonstrate that the distinct receptor behaviours and signalling dynamics observed may be primarily driven by differences in ligand–receptor affinity. Furthermore, our results provide a clear rationale for the different mechanisms of pathway regulation found *in vivo* for each of these growth factors.

INTRODUCTION

The transforming growth factor β (TGF-β) family of ligands plays diverse roles in embryonic development and adult tissue homeostasis, and moreover, their signalling is deregulated in a range of human diseases, including cancer (Massagué, 2008; Pickup et al., 2017). The mammalian TGF-β family consists of 33 members, which signal via the same conserved mechanism (Moses et al., 2016). Two classes of cell surface serine/threonine kinase receptors, termed type I and type II, recognise TGF-β family ligands. Ligand binding brings the receptors together, allowing the constitutively active kinase of the type II receptor to phosphorylate the type I receptor. This both activates the type I receptor, and provides a binding site for the intracellular effectors of the pathways, the SMADs (Heldin and Moustakas, 2016). The receptor-regulated SMADs (R-SMADs) become phosphorylated at their extreme C-termini by the type I receptor, and this drives the formation of complexes with the

[1]Developmental Signalling Laboratory, The Francis Crick Institute, 1 Midland Road, London NW1 1AT, UK. [2]Karolinska Institutet, Department of Medical Biochemistry and Biophysics and SciLifeLab Biomedicum 9B, Solnavägen 9, SE-171 65 Solna, Stockholm, Sweden.
*Present address: Institute of Cancer Research, 15 Cotswold Road, Sutton SM2 5NG, UK.

‡Author for correspondence (caroline.hill@crick.ac.uk)

C.S.H., 0000-0002-8632-0480

common mediator SMAD, SMAD4. These complexes accumulate in the nucleus where they regulate the transcription of a battery of target genes in conjunction with specific co-factors. The TGF-β family has traditionally been split into two pathways, with the TGF-βs, NODAL and activin leading to the phosphorylation of SMAD2 and SMAD3 (SMAD2/3), whereas the BMPs and some of the GDF proteins induce phosphorylation of SMAD1, SMAD5 and SMAD9 (SMAD1/5/9) (Schmierer and Hill, 2007). This, however, is a simplification, as some ligands, in particular TGF-β and activin, can activate both signalling arms (Daly et al., 2008; Hatsell et al., 2015; Ramachandran et al., 2018).

TGF-β receptors are known to internalise in the absence and presence of ligand, and once activated, to signal from early endosomes (Di Guglielmo et al., 2003; He et al., 2015; Miller et al., 2018; Mitchell et al., 2004). A proportion of internalised receptors have been shown to recycle constitutively back to the cell surface, while the remainder are targeted for degradation (Le Roy and Wrana, 2005; Yakymovych et al., 2018). Although the mechanisms underlying the immediate cellular response to TGF-β family ligands is relatively well understood, the response to longer durations of ligand exposure, and the resulting dynamics of signalling, have been much less studied. All the mammalian TGF-β family ligands signal through just seven type I and five type II receptors, so the wide range of cell behaviours seen in response to different ligands are likely to involve additional levels of complexity, some of which will be at the level of signalling dynamics. Because cells are exposed to TGF-β family ligands for extended durations during embryonic development and in disease states (Hill, 2018; Miller and Hill, 2016; Schier and Talbot, 2005), as well as in the context of regenerative medicine (Pagliuca et al., 2014), it is crucial to understand how long-term exposure to ligands is regulated. This will be essential for identifying potential novel points of intervention in each pathway, both experimentally and for the development of therapeutic strategies. Moreover, as all TGF-β family ligands result in the phosphorylation of just two classes of R-SMAD, understanding whether particular ligands lead to different dynamic patterns of SMAD phosphorylation, and how these are regulated, is critical for our understanding of how these pathways evolved and diverged.

We have previously shown that in response to the continuous presence of TGF-β, cells enter a refractory state where they no longer respond to acute TGF-β stimulation. This is due to the rapid depletion of receptors from the cell surface in response to ligand (Vizan et al., 2013). This means that intracellular signalling downstream of TGF-β (as read out, for example, by levels of phosphorylated R-SMADs) is not proportional to the duration of signalling, neither is it sensitive to the presence of ligand antagonists in the extracellular milieu. This type of behaviour would clearly be incompatible with the ability of ligands like BMPs, NODAL and activin to act as morphogens that signal over many cell diameters in the context of embryonic development and tissue homeostasis

(Hedger and de Kretser, 2013; Langdon and Mullins, 2011). We thus postulated that these other TGF-β family ligands might respond to prolonged ligand exposure in a different manner to TGF-β.

We set out to directly test this hypothesis by fully characterising the response of cells to prolonged activin and BMP4 stimulation. Our results show that in contrast to what is seen with TGF-β, cells integrate their response to BMP4 and activin over time, and do not enter a refractory state when stimulated with these ligands. Moreover, we observe an oscillatory SMAD1/5 phosphorylation in response to BMP4 stimulation, which we show is driven by the transient expression of the I-SMADs, SMAD6 and SMAD7, which leads to a temporary depletion of receptors from the cell surface. By combining our experimental insights with mathematical modelling, we can explain these distinct behaviours of activin, BMP4 and TGF-β as being the result of differences in trafficking of their cognate receptors and differential affinities of ligands for their receptors. This in turn may explain the distinct functional roles these ligands play *in vivo*.

RESULTS
BMP4 and activin exhibit distinct patterns of signalling dynamics

We have previously shown that when cells are stimulated with TGF-β, SMAD2 phosphorylation peaks after 1 h, before attenuating to lower levels. After an initial acute response, cells are refractory to further acute stimulation due to an almost complete depletion of receptors from the cell surface (Vizan et al., 2013). To understand whether this was a common feature of all TGF-β family ligands, we characterised the response of cells to other members of the TGF-β family, namely activin A and BMP4, and compared and contrasted them with each other and with TGF-β. For the activin responses, we

predominantly used the P19 mouse teratoma cell line, as SMAD2 is robustly phosphorylated in response to activin in this cell line (Coda et al., 2017). Activin signalling in these cells is mediated by ACVR1B as the type I receptor, and either ACVR2A or ACVR2B as the type II receptors, as demonstrated by the abrogation of signalling when these receptors are knocked down by siRNA (Fig. S1). These cells also produce and secrete the TGF-β family ligands NODAL and GDF3, resulting in a relatively high level of basal phosphorylated SMAD2 (PSMAD2) (Coda et al., 2017). To characterise the BMP4 responses, we predominantly used the human breast cancer cell line MDA-MB-231 and the mouse fibroblast cell line NIH-3T3, both of which induce robust SMAD1/5 phosphorylation in response to BMP4. In addition, we used HaCaT cells, the cell line we previously used to characterise TGF-β signalling dynamics (Vizan et al., 2013).

In response to continuous stimulation with BMP4, SMAD1/5 phosphorylation in MDA-MB-231 cells peaked after 1 h, then dropped down to a lower level after 4 h, before increasing back up to its maximal level after 8 h of stimulation (Fig. 1A). This is strikingly different to the dynamics of signalling seen in response to TGF-β, where chronic exposure of cells to ligand leads to signal attenuation resulting in a low level of SMAD2 phosphorylation (Vizan et al., 2013). A similar single oscillation is evident when NIH-3T3 cells (Fig. S2A) or human keratinocyte HaCaT cells (Fig. S2B) are stimulated with BMP4, although NIH-3T3s reach their low point of signalling after 2 h of stimulation, rather than 4 h, and in neither of these cell types does the signal return to the maximal level, as it does in the MDA-MB-231 cells. The long-term response to activin is different. P19 cells exhibit a high level of basal PSMAD2 as a result of the production of NODAL and GDF3 (Coda et al., 2017),
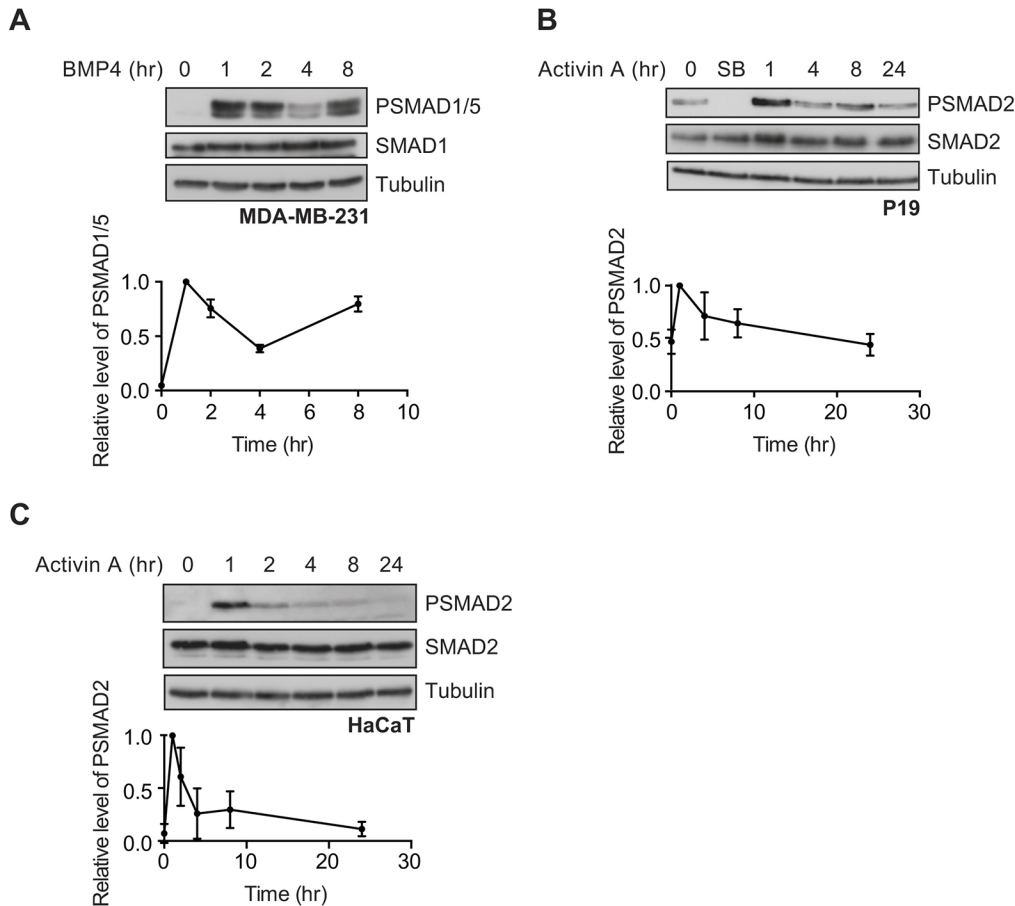

Fig. 1. BMP4 and activin signal with distinct dynamics. (A) MDA-MB-231 cells were treated with BMP4 for the times indicated. (B,C) P19 cells (B) or HaCaT cells (C) were treated with activin A for the times indicated or SB-431542 (SB) overnight. Western blotting for PSMAD1/5, SMAD1, PSMAD2, SMAD2/3 and tubulin, as a loading control, was performed. Quantifications are normalised mean ±s.d. of densitometry measurements from three independent experiments, which are normalised to measurements in cells treated with growth factors for 1 h.

which is completely abolished by overnight incubation with the type I receptor inhibitor SB-431542 (Inman et al., 2002a) (Fig. 1B). When stimulated with activin, P19 cells exhibited maximal levels of PSMAD2 after 1 h, which was modestly attenuated down to the basal level over the next 24 h (Fig. 1B). P19 cells can also be induced by activin from the SB-431542-inhibited baseline, and in this case, show a very sustained response, due to the autocrine production of NODAL and GDF3 (Coda et al., 2017). In HaCaT cells, in contrast, the baseline of PSMAD2 is low and the activin response is more transient, likely because HaCaT cells do not exhibit autocrine signalling (Fig. 1C).

Activin and BMP4 signalling is integrated over time

We next sought to determine whether signalling by activin and BMP4 is integrated over time after stimulation, and compared the behaviours with that seen for TGF-β. Cells were therefore stimulated for increasing periods of time with activin, BMP4 or TGF-β, and

then chased for the remainder of the 1 h with saturating doses of the natural ligand antagonists for activin and BMP4, follistatin (Nakamura et al., 1990) and noggin (Zimmerman et al., 1996), respectively, or, in the case of TGF-β, the neutralising antibody 1D11 (Nam et al., 2008) (Fig. 2A). All cells were harvested together at the 1 h time point. TGF-β induced a maximal PSMAD2 response after just 5 min of exposure to ligand (Fig. 2B), which we have previously demonstrated is due to the rapid depletion from the cell surface of the type II TGF-β receptor TGFBR2 within this time frame, so that little to no new signalling is induced over the remainder of the first hour of signalling (Vizan et al., 2013). In contrast, the cellular response to activin is integrated over the first hour of signalling, with a greater induction of PSMAD2 resulting from longer exposure to ligand (Fig. 2C,D). A similar pattern was observed with SMAD1/5 phosphorylation resulting from BMP4 stimulation in MDA-MB-231 cells (Fig. 2E) and HaCaT cells (Fig. 2F). We conclude that cells continuously monitor the presence
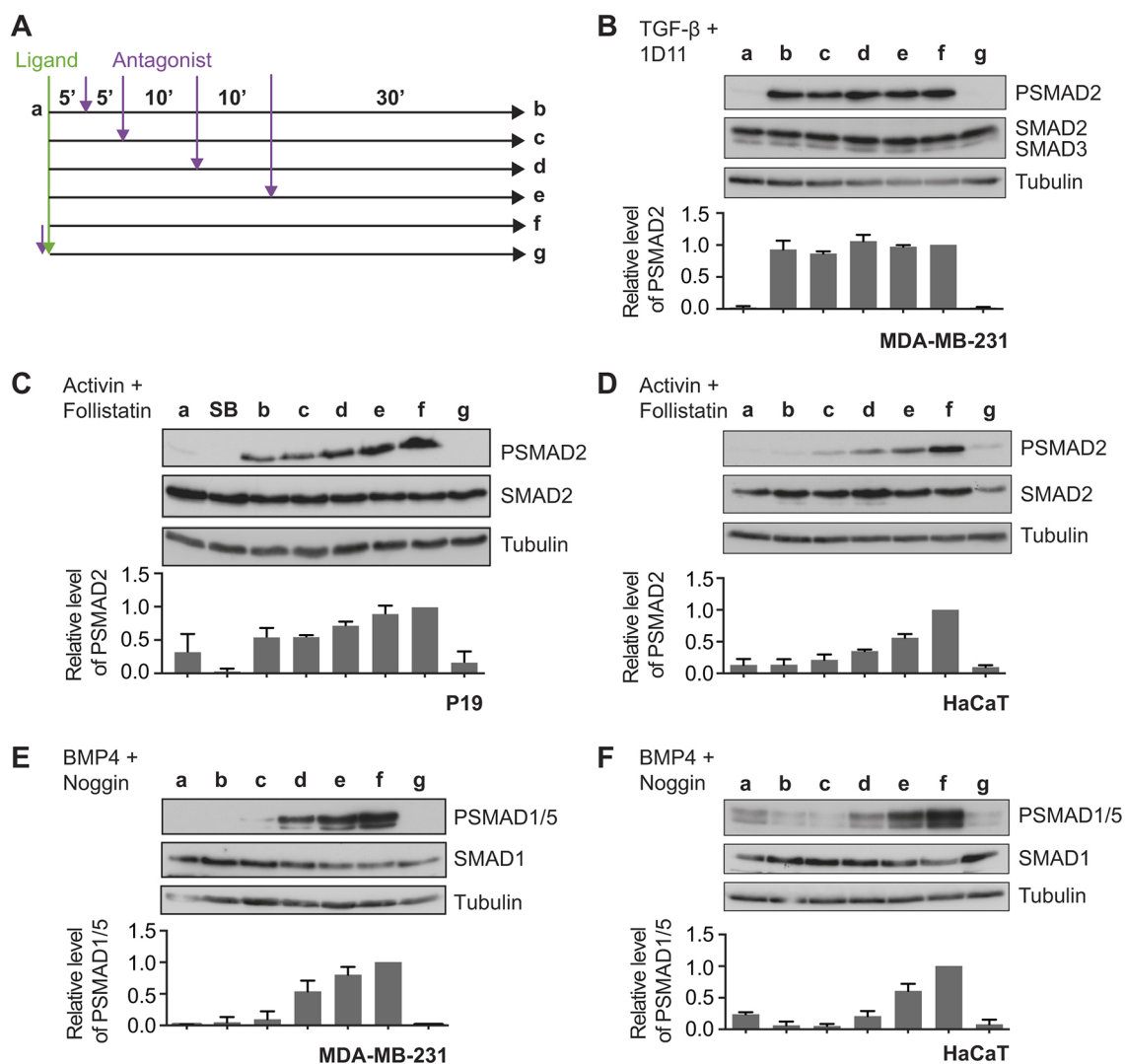

Fig. 2. Activin and BMP4 signals are integrated over time, whereas TGF-β signals are not. (A) Experimental scheme. Cells were untreated (a), or treated with ligand for 5 (b), 10 (c), 20 (d), 30 (e), or 60 (f) min, followed by the cognate ligand antagonist for the remainder of 60 min. To ensure that inhibitors were working as expected, cells were pre-treated with inhibitor for 5 min, followed by ligand for 60 min (g). (B) MDA-MB-231 cells were treated as in A with TGF-β and the blocking antibody, 1D11. (C) P19 cells were treated as in A with activin and follistatin, and additionally overnight with SB-431542 (SB). (D) HaCaT cells were treated as in A with activin and follistatin. (E) MDA-MB-231 cells were treated as in A with BMP4 and noggin. (F) HaCaT cells were treated as in A with BMP4 and noggin. Western blotting for PSMAD1/5, SMAD1, PSMAD2, SMAD2/3 and tubulin, as a loading control, was performed. Quantifications are means±s.d. of densitometry measurements from three independent experiments, which are normalised to measurements in cells treated with growth factors for 1 h.

of BMP4 and activin in their extracellular environment, such that the R-SMAD phosphorylation observed after 1 h in response to BMP and activin is an integration of all of the signalling that has occurred in the first hour. This behaviour is distinct from that seen with TGF-β, where the SMAD phosphorylation after 1 h of stimulation is the result of the first 5 min of ligand exposure.

Stimulation with activin and BMP4 does not induce refractory behaviour

We have previously shown that cells enter a refractory state in response to TGF-β treatment, where they are unable to respond to acute stimulation with the same ligand. To determine whether the same state is induced in response to activin and BMP4, cells were stimulated with these ligands for 1 h, followed by treatment with ligand antagonists for 2 h to reduce R-SMAD phosphorylation levels back down to basal levels. The ligand antagonists were then washed out and cells re-stimulated with ligand for 1 h. The efficacy of the ligand antagonists and their wash-out was confirmed (lanes g and f, respectively, in Fig. 3A, and lanes h and g, respectively, in Fig. 3B). For both BMP4 (Fig. 3A) and activin (Fig. 3B), re-stimulation to maximal PSMAD levels was observed after just 2 h treatment with ligand antagonists, indicating that cells do not
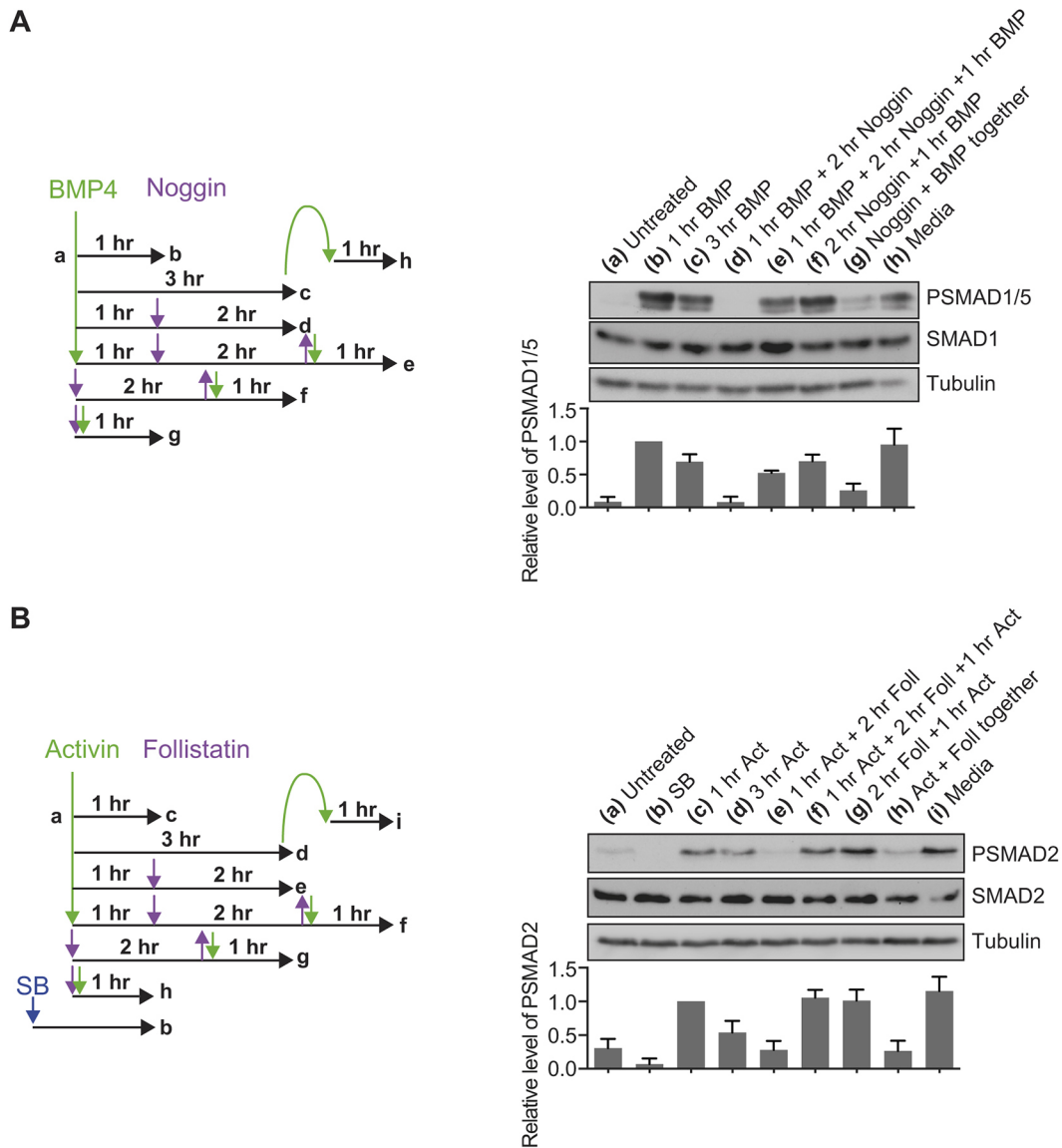

Fig. 3. BMP4 and activin do not induce refractory behaviour. (A) Left, a schematic of the experimental set-up. NIH-3T3 cells were untreated (a) or treated with BMP4 for 1 h (b) or 3 h (c). After 1 h of BMP4 stimulation, the signal was brought down to baseline through treatment with noggin for 2 h (d), which was then washed out and cells were re-stimulated with BMP4 for 1 h (e). The efficacy of noggin washout was confirmed (f), as was its inhibitory ability by adding the ligand and antagonist simultaneously (g). To confirm that BMP4 was not depleted from the medium in the time period of these experiments, cells were stimulated with BMP4 for 3 h, then the medium transferred to naïve cells for 1 h (h). Right, western blotting for PSMAD1/5, SMAD1 and tubulin, as a loading control, was performed. Quantifications are means±s.d. of densitometry measurements from three independent experiments, which are normalised to measurements in cells treated with BMP4 for 1 h. (B) Left, a schematic of the experimental set-up. P19 cells were untreated (a), treated overnight with SB-431542 (b) or treated with activin for 1 h (c) or 3 h (d). After 1 h of activin stimulation, the signal was brought down to baseline through treatment with follistatin for 2 h (e), which was then washed out and cells were re-stimulated with activin for 1 h (f). The efficacy of follistatin washout was confirmed (g), as was its inhibitory ability (g). To confirm that activin was not depleted from the medium in the time period of these experiments, cells were stimulated with activin for 3 h, then the medium transferred to naïve cells for 1 h (i). Right, western blotting for PSMAD2, SMAD2 and tubulin, as a loading control, was performed. Quantifications are means±s.d. of densitometry measurements from three independent experiments, which are normalised to measurements in cells treated with activin for 1 h.

enter a refractory state in response to these ligands. This contrasts with the behaviour of cells stimulated with TGF-β. In this case, cells take 12–24 h after the removal of external ligand to recover the ability to fully respond again to ligand (Vizan et al., 2013).

The distinct signalling dynamics of TGF-β, activin and BMP4 are not explained by the intracellular lifetimes of their receptors

TGF-β family receptors can signal from internal cellular compartments (Itoh et al., 2002), and we have shown that the lifetime of receptors in these compartments is likely to be an important factor for regulating the dynamics of signalling (Vizan et al., 2013). We therefore determined whether the distinct signalling dynamics observed in response to each ligand could be driven by the duration for which activated receptors signal from internal compartments.

To address this, cells were stimulated for 1 h with TGF-β, BMP4 or activin, then chased over a time course of 8 h with the cognate ligand antagonists 1D11, noggin and follistatin, respectively, and the levels of R-SMAD phosphorylation were assayed (Fig. 4). Because there is no new signalling induced by the activation of receptors with external ligands once antagonists are added, any on-going PSMAD signal must arise from the combined activities of the receptors signalling from internalised compartments and cellular R-SMAD phosphatases. To control for the latter, the decay in R-SMAD phosphorylation due to the action of R-SMAD phosphatases was assayed directly by chasing stimulated cells with receptor kinase inhibitors SB-431542 (for TGF-β and activin) or LDN-193189 (for BMP4; Cuny et al., 2008) over the same time course. By comparing the decay in signal seen with ligand antagonists versus receptor kinase inhibitors, the duration of signalling from internal compartments can be determined. In the presence of the kinase inhibitors, maximal R-SMAD dephosphorylation occurred within ~30 min in all cases (Fig. 4B–D), with a half-life of ~15 min, as determined by fitting an exponential decay curve to the data. In contrast, in the presence of ligand antagonists, the signal in response to TGF-β decayed with a half-life of ~52 min, the signal from BMP4 in ~44 min and that from activin in ~42 min (Fig. 4B–D). Thus, signalling persists for ~2 h in all cases, suggesting that receptors signal from endosomes for ~90 min, with no obvious differences seen between the different ligands.

Receptor trafficking behaviours drive distinct signalling dynamics for the different ligands

We reasoned that differences in signalling dynamics could be driven by differences in the behaviour of the receptors for each ligand. Antibodies for western blotting were validated against one of the BMP4 type II receptors, BMPR2 (Daly et al., 2008), the activin type I receptor ACVR1B (formerly known as ALK4) and ACVR2B (Tsuchida et al., 2009). In all cases, PNGase treatment, which removes N-linked sugars, resulted in an increased mobility of the receptors, and siRNA knockdown was used to confirm the specificity of the antibodies and the identity of the correct band (Fig. S3A–C). No antibodies against BMP type I receptors were identified that could detect endogenous expression (data not shown).

We next determined the half-life of each receptor species to which we had antibodies. Cycloheximide chase time course assays were performed, which showed that BMPR2 has a half-life of ~4 h (Fig. S3D) and ACVR1B of ~1 h (Fig. S3E). ACVR2B was not noticeably degraded at all over the time course in either P19 (Fig. S3F) or HaCaT (Fig. S3G) cells, indicating that it has a much longer half-life than the other receptors tested. The half-lives of BMPR2 and ACVR1B are of the same order as those previously

calculated for the TGF-β receptors (~2 h for TGFBR2 and ~4 h for TGFBR1; Vizan et al., 2013).

We have previously shown that TGFBR1 and TGFBR2 are rapidly depleted from the surface of cells in response to TGF-β stimulation (Vizan et al., 2013). We therefore wanted to know whether BMP and activin stimulation similarly drives receptor depletion, and performed surface biotinylation assays on cells treated with BMP4 or activin to test this. In MDA-MB-231 cells, BMPR2 was depleted from the cell surface after 2 h of BMP4 treatment, before re-accumulating at later time points (Fig. 5A). Although receptors re-accumulated, they did not appear to fully reach their level in unstimulated cells. Receptor depletion and re-accumulation occurred with similar dynamics to the oscillation in PSMAD1/5 levels seen in response to signal. Despite the transient depletion of BMPR2, in response to long-term stimulation, it remained present at the cell surface. This explains why cells do not become refractory to further acute stimulation after treatment with BMP4.

By contrast, in P19 cells, we could show that neither ACVR1B nor ACVR2B were depleted from the cell surface in response to activin or in the presence of the receptor inhibitor SB-431542 (Fig. 5B). As a control for visualisation of a cell surface protein whose levels change in response to signal, we assessed the cell surface levels of the NODAL/GDF co-receptor TDGF1, whose expression is upregulated in response to activin signalling. TDGF1 robustly accumulated in response to activin both at the cell surface and in whole-cell lysates (Fig. 5B). Again, the constant presence of activin receptors at the cell surface during ligand stimulation explains why cells do not enter a refractory state after an acute activin induction. Cells thus remain competent to respond to acute doses of ligand in their extracellular environment, even after an initial stimulation with activin.

The oscillatory response to BMP4 depends on the continuous presence of BMP4 in the extracellular milieu and requires new protein synthesis

Stimulation with BMP4 leads to an oscillatory PSMAD1/5 response driven by receptor depletion and re-accumulation. This oscillatory behaviour is visible in multiple cell lines from different species, including NIH-3T3, MDA-MB-231 and HaCaT cells, although they show slightly different time points at which PSMAD1/5 reaches its lowest level, and they recover to different extents (Fig. 1; Fig. S2). Because NIH-3T3 cells exhibited the most robust oscillation, they were used for subsequent experiments. To determine whether the second wave of signalling after the dip in PSMAD1/5 is a result of new receptor activation at the cell surface or a second wave of signalling from internalised receptors, cells were stimulated for 1 h with BMP4, which was subsequently washed out (Fig. S4A) or neutralised with noggin (Fig. S4B). In both cases, no second wave of signalling was seen, indicating that the continuous presence of BMP4 in the medium is necessary for the second increase in PSMAD1/5 observed after an initial decrease.

One possible explanation for these oscillatory dynamics is that another TGF-β family ligand, such as TGF-β itself, could be playing a role, possibly as a feedback target of the pathway that could be negatively regulating SMAD1/5 phosphorylation (Gronroos et al., 2012). To exclude this possibility, at least for a large subset of ligands that signal through SMAD2/3, BMP4 signalling was assessed by looking at PSMAD1/5 levels over time courses in the presence and absence of the TGF-β, activin and NODAL receptor inhibitor SB-431542 (Fig. S4C). However, no differences in PSMAD1/5 dynamics in response to BMP4 were seen in the presence or absence of SB-431542, ruling out such a feedback
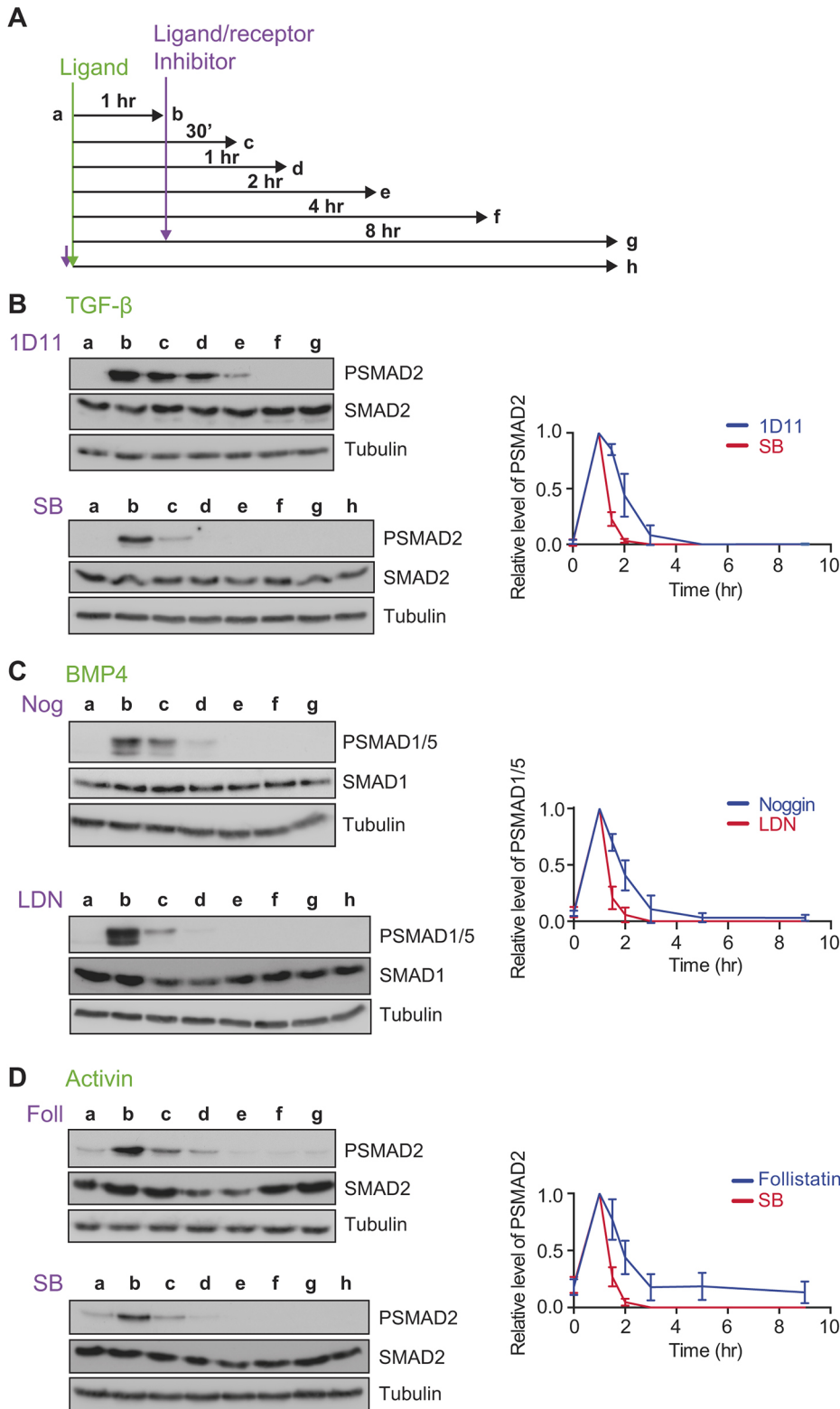
Fig. 4. The distinct TGF-β, activin and BMP4 signalling dynamics are not explained by the intracellular lifetimes of their receptors. (A) Experimental scheme. Cells were untreated (a), or treated for 1 h with ligand (b), then with ligand antagonist or receptor kinase inhibitors for 30 mins (c), 1 h (d), 2 h (e), 4 h (f) or 8 h (g), or with ligand and receptor kinase inhibitor together for 8 h (h). (B) MDA-MB-231 cells were treated as in A with TGF-β, 1D11 or SB-431542 (SB). (C) MDA-MB-231 cells were treated as in A with BMP4, noggin (Nog) or LDN-193189 (LDN). (D) P19 cells were treated as in A with activin A, follistatin (Foll) or SB-431542 (SB). Western blotting for PSMAD1/5, SMAD1, PSMAD2, SMAD2/3 and tubulin, as a loading control, was performed. Quantifications are means±s.d. of densitometry measurements from three independent experiments, which are normalised to measurements in cells treated with growth factors for 1 h.

mechanism, whereby PSMAD1/5 would be upregulating or activating a different TGF-β family ligand.

We also investigated whether protein synthesis was required for the oscillatory behaviour. Time courses of BMP4 treatment were performed in the presence or absence of the translation inhibitor, cycloheximide. In the presence of cycloheximide, no oscillation in PSMAD1/5 levels was observed and levels remained high throughout the time course (Fig. S5A). This indicates that a negative regulator of the pathway must be expressed in response to signalling, and that this factor is responsible for oscillatory PSMAD1/5 dynamics. To confirm this, time courses of BMP4 treatment were performed in the presence of the transcriptional inhibitor actinomycin D (Fig. S5B). Again, the dip in PSMAD1/5 levels seen in control cells is abrogated in the absence of new transcription.
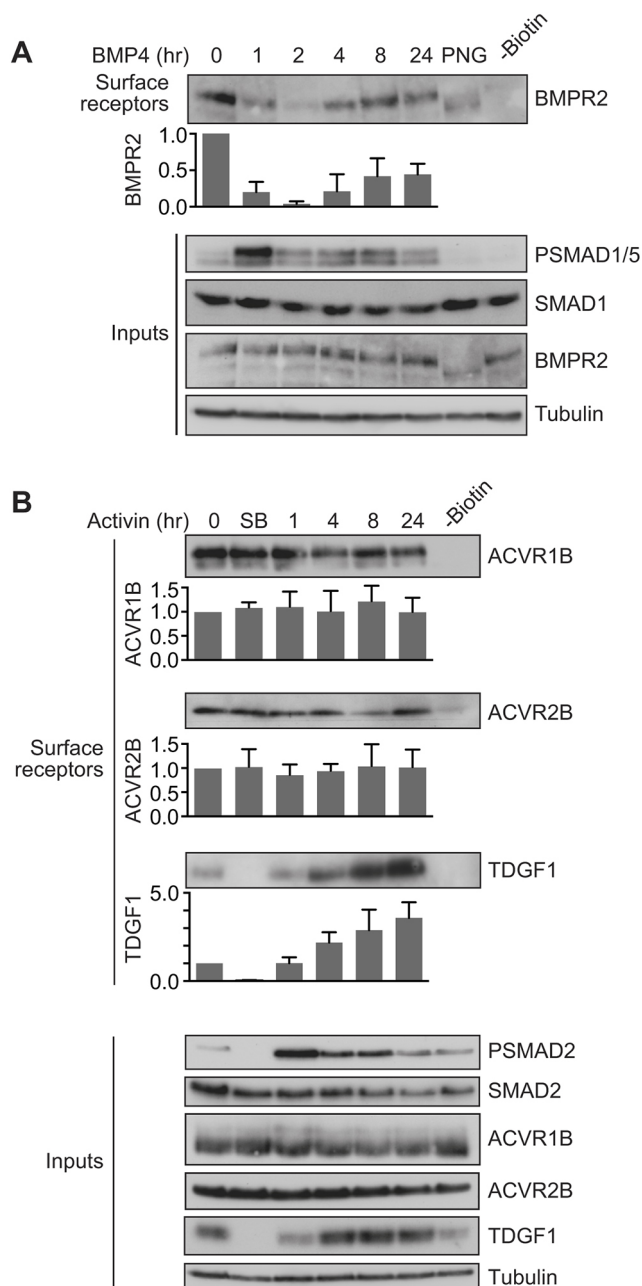
Fig. 5. BMP4 and activin drive distinct receptor trafficking behaviours. (A) MDA-MB-231 cells were treated with BMP4 for the times indicated. (B) P19 cells were treated with activin for the times indicated or with SB-431542 overnight (SB). Whole-cell extracts were western blotted for BMPR2, PSMAD1/5, SMAD1, ACVR1B, ACVR2B, TDGF1, PSMAD2 and SMAD2/3, with tubulin as a loading control (Inputs). Surface biotinylation assays were performed to isolate surface receptor populations, which were western blotted for BMPR2, ACVR1B, ACVR2B and TDGF1. For the lane marked –Biotin, unstimulated cell extracts were treated identically to the other samples, but without the addition of biotin. In A, the lane marked PNG corresponds to a 0 time point where the sample was treated with PNGase to remove N-linked sugars from the receptors prior to gel electrophoresis. Quantifications are the normalised mean±s.d. of densitometry measurements from three independent experiments, relative to the levels in untreated cells.

The oscillatory response to BMP4 requires the inhibitory SMADs, SMAD6 and SMAD7

Two of the most likely candidates to be feedback inhibitors of BMP signalling are the inhibitory SMADs (I-SMADs), SMAD6 and

SMAD7. Both I-SMADs have long been known to be targets of BMP signalling (Takase et al., 1998) and are negative regulators of the pathway. Several mechanisms for their inhibitory activity have been proposed, including interfering with SMAD complex formation (Hata et al., 1998), inhibiting R-SMAD phosphorylation (Hayashi et al., 1997; Imamura et al., 1997; Nakao et al., 1997), targeting receptors for degradation (Ebisawa et al., 2001; Kavsak et al., 2000) and blocking the DNA-binding and transcriptional activity of the SMADs (Lin et al., 2003). In NIH-3T3 cells, quantitative (q)PCR revealed that in response to BMP4 stimulation, Smad6 and Smad7 mRNAs are both induced in a transient manner that is the exact inverse of the PSMAD1/5 signal for Smad6, and in phase with PSMAD1/5 signal for Smad7 (Fig. 6A). siRNA-mediated knockdown of Smad6 and Smad7 (siSmad6/7) together abrogated the oscillation in PSMAD1/5 levels seen with control, non-targeting (siControl) siRNAs (Fig. 6B). Antibodies against endogenous SMAD6 and SMAD7 could not be identified, so knockdown of these genes was confirmed at the level of mRNA. Individual siRNA pools against Smad6 and Smad7 both abolished oscillations in PSMAD1/5, although knockdown of Smad7 led to a weaker PSMAD1/5 response and a reduction in total SMAD1 levels (Fig. S5C).

To confirm that these results apply across cell lines from different species, the dynamics of expression of SMAD6 and SMAD7 in response to BMP4 in MDA-MB-231 cells were also examined. SMAD6 was induced after 2 h of BMP4 stimulation and stayed elevated over the duration of an 8-h time course, while SMAD7 showed a transient peak of expression after 2 h, then declined down to a lower level (Fig. S6A). Knockdown of SMAD6 and SMAD7 together in MDA-MB-231 cells abrogated the PSMAD1/5 oscillation in a similar way to that observed in NIH-3T3 cells (Fig. S6B), indicating that this mechanism is conserved across species.

SMAD6 and SMAD7 are required for the transient depletion of BMPR2 from the cell surface

SMAD6 and SMAD7 have been described to target TGF-β superfamily receptors for degradation (Ebisawa et al., 2001; Goto et al., 2007; Kavsak et al., 2000). We therefore reasoned that the transient peak in their expression in response to BMP4 could be responsible for the transient depletion of BMP receptors from the cell surface, leading to the subsequent dip in SMAD1/5 phosphorylation. To test this, surface biotinylation assays were performed in NIH-3T3 cells transfected with either control non-targeting siRNAs or siRNAs against Smad6 and Smad7. The BMPR2 receptor also transiently depleted and re-accumulated in this cell line in response to BMP4 stimulation, indicating that this mechanism is conserved across species (Fig. 6C). Upon knockdown of SMAD6 and SMAD7, BMPR2 was no longer transiently depleted from the cell surface in response to BMP4, but remained at high levels throughout the time course, indicating that a failure to deplete receptors from the cell surface in the absence of SMAD6 and SMAD7 underlies the lack of oscillation in SMAD1/5 phosphorylation in this condition (Fig. 6C).

Using mathematical modelling to find the key parameters that dictate specific signalling dynamics

To obtain clues as to key parameters that might explain the distinct signalling dynamics of the different ligands, we took a mathematical modelling approach. We previously built a mathematical model of the TGF-β pathway that simulated the refractory behaviour of the TGF-β ligand (Vizan et al., 2013). This model itself was an extension of our previous model describing the intracellular signalling module of the TGF-β pathway (Schmierer et al., 2008). Implementing our 2013
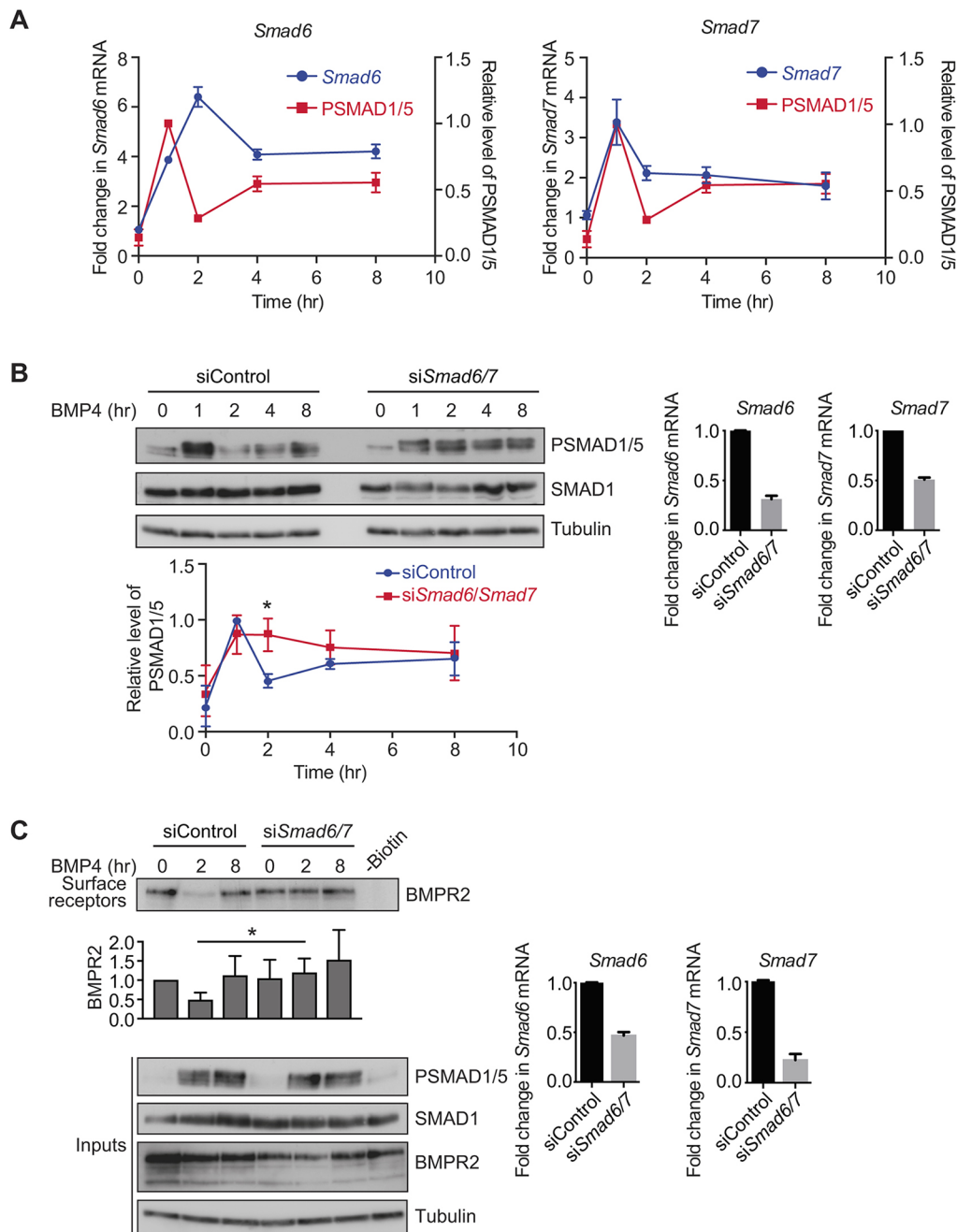
Fig. 6. SMAD6 and SMAD7 are required for the oscillatory signalling response to BMP4. (A) NIH-3T3 cells were treated with BMP4 for the times indicated. Levels of *Smad6* and *Smad7* mRNA were assayed by qPCR. Shown are the normalised means and s.d.s from three independent experiments, expressed as fold change in mRNA level relative to the levels in untreated cells, overlaid with SMAD1/5 phosphorylation data from Fig. S2. (B) NIH-3T3 cells were transfected with non-targeting control siRNAs (siControl) or siRNA SMARTpools targeting *Smad6* and *Smad7* (si*Smad6/7*), and were then treated with BMP4 for the times indicated. Western blotting for PSMAD1/5, SMAD1 and tubulin was performed. Quantifications are means±s.d. of densitometry measurements from three independent experiments, which are normalised to measurements in siControl cells treated with BMP4 for 1 h. *P<0.05. The extent of knockdown was determined by qPCR. Shown are the normalised mean±s.d. from three independent experiments, expressed as the fold change in mRNA level relative to that in non-targeting controls. (C) NIH-3T3 cells were transfected with non-targeting control siRNAs or siRNA SMARTpools targeting *Smad6* and *Smad7*, and were then treated with BMP4 for the times indicated. A biotinylation assay was performed to isolate surface receptor populations, which were western blotted for BMPR2. Input cell lysates were also western blotted for BMPR2, PSMAD1/5, SMAD1 and tubulin, as a loading control. For the lane marked –Biotin, unstimulated cell extracts were treated identically to the other samples, but without the addition of biotin. Quantifications are the normalised mean±s.d. of densitometry measurements from three independent experiments, relative to the levels in untreated siControl cells. *P<0.05. The extent of knockdown was determined by qPCR. Shown are the normalised mean±s.d. from three independent experiments, expressed as fold change in mRNA level relative to non-targeting controls.

model as a starting point, we used our experimental findings, as well as the published literature, to determine whether, by changing some key parameters, we could simulate the signalling dynamics of activin and BMP4 that we observed experimentally.

A striking difference between TGF-β itself and the other TGF-β family ligands is that TGF-β binds its receptors cooperatively, whereas there is no evidence for cooperativity in receptor binding for BMP4 and activin (Groppe et al., 2008; Hinck, 2012). This

likely explains the higher affinity measured for TGF-β1 and TGF-β3 for their receptors (K_d=5–30 pM) (De Crescenzo et al., 2003; Massagué, 1990), compared with the lower affinities measured for BMP4 and activin with their cognate receptors (K_d=110 pM for BMP4 and 100–380 pM for activin) (Attisano et al., 1992; Luyten et al., 1994).

Starting first with the activin pathway, we used our model to investigate whether lowering the affinity of activin for its receptors would result in the distinct behaviours we have measured for activin signalling versus TGF-β signalling. We found that implementing the published value (365 pM) for the K_d of activin for its receptors, and making minor adjustments to several other parameters (see Materials and Methods section) resulted in the model converting from simulating the characteristic behaviours of TGF-β signalling into simulating those of activin. The modified model faithfully captured the long-term activin dynamics both in cells with no basal signalling, like HaCaT cells, or with basal signalling, like P19 cells (Fig. 7A). The simulations also reproduced the observed integration of signalling over time (Fig. 7B), the behaviour of the pathway when receptors are inhibited with a small-molecule inhibitor or when ligand is neutralised with follistatin (Fig. 7C), and also the ability of the pathway to be re-stimulated after ligand removal (Fig. 7D).

BMP4 signalling dynamics are similar to those of activin in the long term, but additionally show oscillatory behaviour in the short term. We have shown that SMAD6 and SMAD7 are required for the oscillation, likely due to their role in inducing activated receptor degradation (Ebisawa et al., 2001; Kavsak et al., 2000). Their effect is transient, because expression of Smad6 and Smad7 in response to BMP4 is transient (Fig. 6A). We used a K_d of 365 pM for BMP4 binding to its receptors (equivalent to that of activin), and additionally included the induction of SMAD6/7 by nuclear PSMAD1–SMAD4 complexes. This was implemented with an RNA intermediate and a non-linear dependency of Smad6/7 expression on activatory PSMAD1–SMAD4 complexes. SMAD6/7 is then assumed to act on the stability of activated receptors (see Materials and Methods for the parameters and details of the modelling). This model captured all the main behaviours of BMP signalling that we observe experimentally, including the oscillation, signal integration over time, the behaviour of the pathway when receptors are inhibited or when ligand is neutralised with noggin, and also the ability of the pathway to be re-stimulated after ligand removal (Fig. 7E–H).
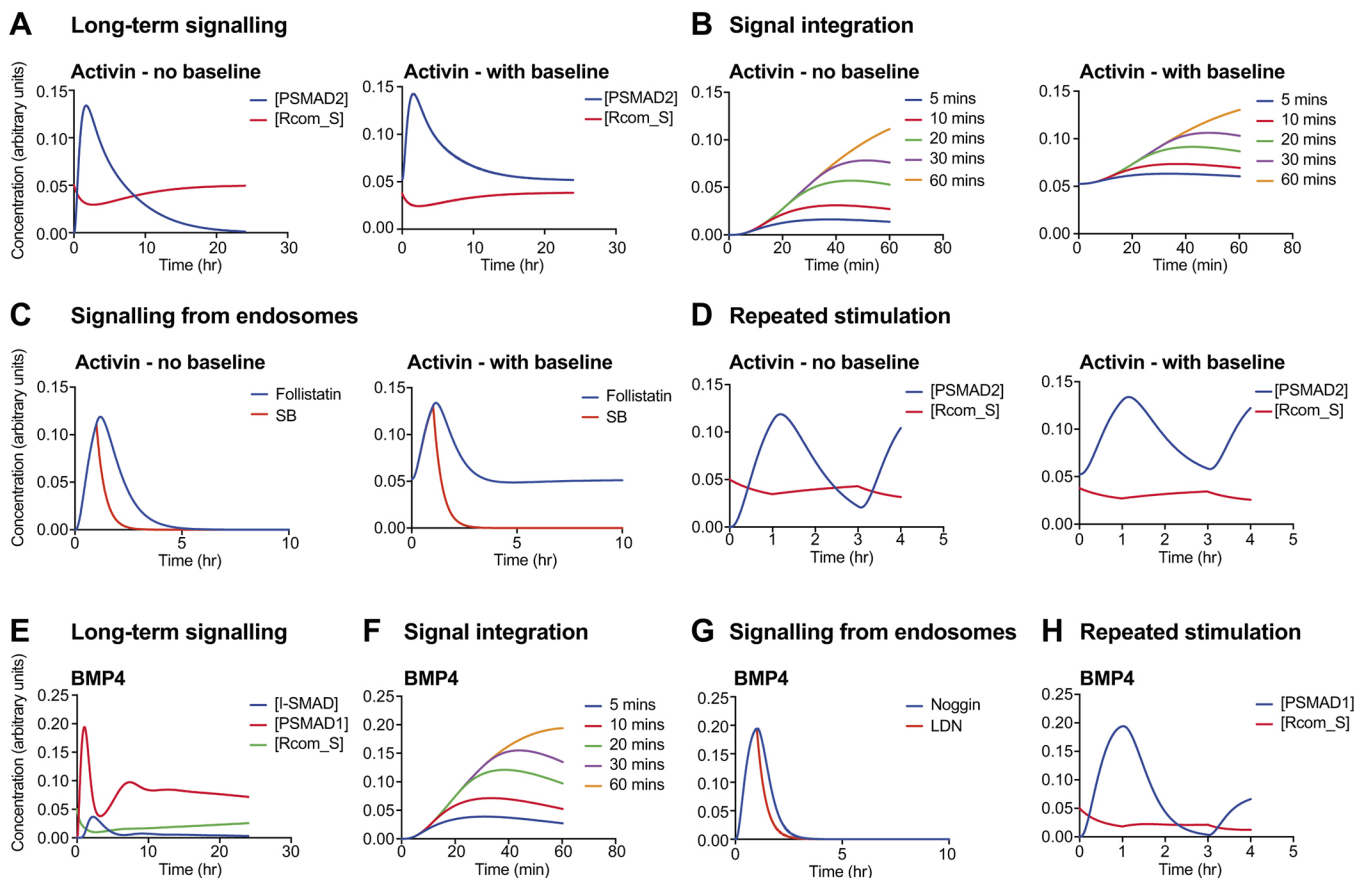

Fig. 7. Mathematical models of the activin and BMP pathways can simulate the experimentally observed behaviours of these ligands. (A–D) The mathematical model described in the text was used to simulate the response of cells to activin. In all cases, responses in cells with no baseline (e.g. HaCaT cells) are shown on the left and responses in a cell line that has a basal level of PSMAD2 signalling (e.g. P19 cells) are shown on the right. (A) Simulation of a long-term activin response; compare with experimental results in Fig. 1C (HaCaT cells) or Fig. 1B (P19 cells). (B) Simulation of the signal integration experiments; compare with Fig. 2D and Fig. 2C, respectively. (C) Simulation of the experiment shown in Fig. 4D, which shows that signalling occurs from intracellular compartments, presumed to be endosomes. (D) Simulation of repeated activin stimulation; compare with Fig. 3B. (E–H) Equivalent simulations were performed for the BMP4 responses. Compare E with Fig. 1A, F with Fig. 2E, G with Fig. 4C, and H with Fig. 3A. In all cases, the concentrations of the indicated species are plotted in arbitrary units. In B and C, PSMAD2 concentration is plotted, and in F and G, PSMAD1 concentration is plotted. R_comS indicates the proportion of signalling competent receptors at the cell surface. SB, SB-431542; LDN, LDN-193189.

DISCUSSION

Receptor trafficking and degradation dictates signalling dynamics for different TGF-β family ligands

In both physiological and pathological contexts *in vivo*, cells are frequently exposed to extracellular ligands for prolonged periods, yet little is currently understood about how cells respond to sustained ligand exposure, or about how signalling dynamics are modulated over time. In this study, we have addressed these questions for members of the TGF-β family of ligands. We have shown that the signalling dynamics differ considerably between activin, BMP4 and TGF-β, and that they are dependent on the localisation and behaviour of cell surface receptors. In contrast to the behaviour of cells treated with TGF-β, cells monitor the presence of activin and BMP4 in the extracellular milieu during signalling, and as a result, signalling is integrated over time. Cells also do not enter a refractory state after an acute stimulation with activin and BMP4, as they do in response to TGF-β. However, while continuous activin stimulation leads to fairly stable SMAD2/3 phosphorylation in P19 cells, owing to the continuous presence of receptors at the cell surface and autocrine signalling, BMP4 stimulation in a number of different cell lines leads to a transient depletion of the receptors from the cell surface due to the transient upregulation of the I-SMADs SMAD6 and SMAD7. This in turn results in an oscillatory signalling response to BMP4, where the response as read out by R-SMAD phosphorylation transiently dips and then recovers.

We therefore propose a model where the dynamics of signalling observed in response to different ligands of the TGF-β superfamily are determined by the localisation and trafficking of cell surface receptors, specifically their rates of internalisation from the cell surface and degradation, and their rates of renewal by recycling and/or new synthesis. At steady state prior to ligand induction, for all receptors, the rate of renewal matches the rate of depletion (Fig. 8A). For TGF-β, ligand addition increases the rate of receptor internalisation and degradation, so receptors become depleted from the cell surface and signalling attenuates (Fig. 8B) (Vizan et al., 2013). For activin, upon ligand addition, depletion is matched by renewal, such that receptors are not depleted from the cell surface. Moreover, the response to ligand is integrated until maximal R-SMAD phosphorylation is reached, and cells do not become refractory to acute stimulation (Fig. 8C). For BMP4, receptor behaviour over the first hour and in the longer term is similar to that for activin, but a transient peak of SMAD6 and SMAD7 expression means that the rate of depletion and/or degradation is greater than the rate of renewal, leading to a transient dip in SMAD1 phosphorylation (Fig. 8D).

Previous models of signalling by TGF-β family ligands have focused on developing a quantitative understanding of how cells respond to individual ligands of the family (for a comprehensive review, see Clarke and Liu, 2008). By comparing and contrasting signalling dynamics across multiple members of the family, our mathematical modelling approach has suggested, for the first time, the importance of ligand affinity for receptors in shaping signalling dynamics. We have shown that we can convert our mathematical model from simulating the refractory behaviour observed for TGF-β to the non-refractory, integrated signalling behaviour observed for activin and BMP, by reducing the affinity of receptors for their ligand, implementing published ligand–receptor dissociation constants (Attisano et al., 1992; De Crescenzo et al., 2003; Luyten et al., 1994; Massagué, 1990). This suggests that the high affinity of TGF-β for its receptors [which is likely, at least in part, to be due to the cooperative interaction between TGF-β and the TGF-β type I and type II receptors (Groppe et al., 2008; Hinck, 2012)], might

explain the dramatic depletion in surface receptors upon TGF-β binding and the subsequent refractory behaviour. In contrast, activin, which has been demonstrated to bind its receptors with lower affinity (Attisano et al., 1992), may not saturate the cell surface receptors, and thus does not cause obvious cell surface receptor depletion. BMP4 also has a lower affinity for its receptors than does TGF-β for its cognate receptors (De Crescenzo et al., 2003; Luyten et al., 1994). Our experimental and modelling results indicate that BMP4 essentially functions like activin, but the activity of the induced SMAD6/7 causes a transient depletion of receptors from the surface and a subsequent dip in PSMAD1/5 levels, giving the characteristic single oscillatory behaviour.

The differences in surface receptor depletion seen in response to TGF-β, BMP4 and activin can also explain the differences in the integration of signalling observed over the first hour after stimulation. The constant presence of BMP and activin receptors at the surface results in a continuous increase in receptor activation over the first hour, such that a longer duration of ligand exposure leads to more receptors being activated. Because the R-SMADs monitor receptor activity as a result of their nucleocytoplasmic shuttling, accumulation of activated receptors results in accumulation of phosphorylated R-SMAD (Schmierer et al., 2008). In the case of TGF-β, receptor activation is maximal after 5–10 min and does not continue to increase with time of ligand exposure.

Distinct TGF-β family signalling dynamics may account for the different *in vivo* roles for these ligands

The differences in signalling dynamics that we have uncovered may account for the distinct roles these ligands play during embryonic development and tissue homeostasis. Activin, and the related ligand NODAL, as well as the BMPs, are well known to form gradients to pattern tissues, and are thought to act as morphogens (Gurdon et al., 1994; Wharton et al., 1993). Crucially, these ligands are all regulated by soluble extracellular ligand antagonists, such as chordin or noggin for BMPs, follistatin for activin, and LEFTY1/2 for NODAL, among others (Brazil et al., 2015; Hedger and de Kretser, 2013; Schier, 2009). The formation of morphogen gradients requires cells to be sensitive to ligand levels at all times, and both the BMP and NODAL gradients formed in early zebrafish embryos have been shown to be shaped by the action of ligand antagonists (Pomreinke et al., 2017; Ramel and Hill, 2013; Schier, 2009; van Boxtel et al., 2015; Zinski et al., 2017).

In contrast to activin, NODAL and BMPs, TGF-β itself has never been shown to act in a gradient during embryonic development. The main roles of TGF-β during early stages of development are in facial morphogenesis (Dudas et al., 2006), heart valve formation (Mercado-Pimentel and Runyan, 2007) and in the development and maintenance of the vascular system (ten Dijke and Arthur, 2007), and graded ligand activity is not apparent in any of these processes. Furthermore, unlike activin, NODAL and the BMPs, TGF-β has no known natural ligand antagonists. Like all the TGF-β family ligands, TGF-β is synthesised as a precursor, with a large pro-domain and a C-terminal mature domain. The mature domain is then cleaved from the pro-domain by proteases of the subtilisin-like pro-protein convertase (SPC) family (Miller and Hill, 2016). This pro-mature complex forms a latent complex with latent TGF-β-binding proteins (LTBPs), and a further activation step is required to release mature TGF-β protein (reviewed in Miller and Hill, 2016). Activin and BMPs are also secreted as pro-mature complexes, but their pro and mature domains are only weakly associated (Mi et al., 2015; Wang et al., 2016). It has been demonstrated for activin that the pro and mature domains have a dissociation constant of ∼5 nM
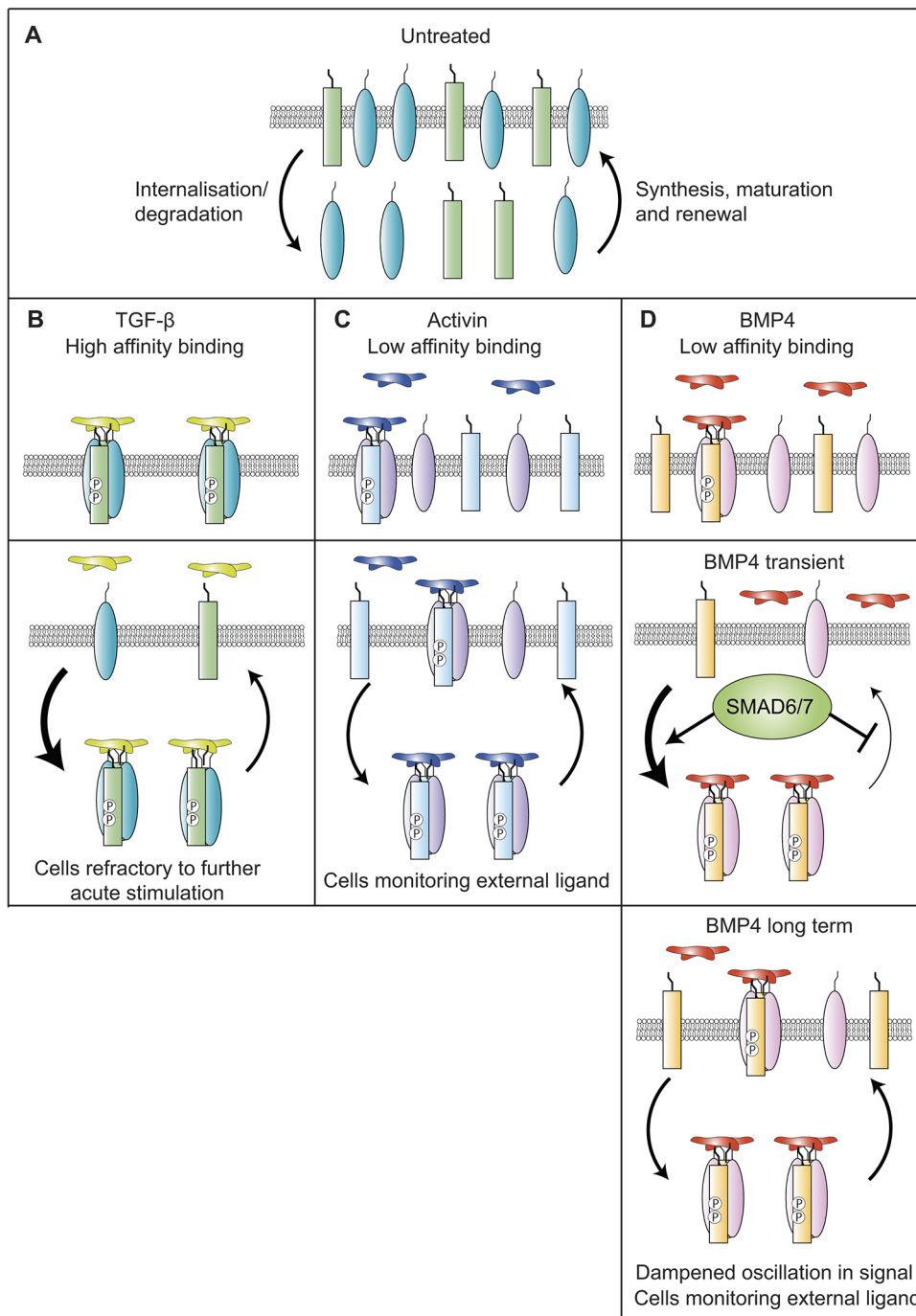
Fig. 8. TGF-β family signalling dynamics are determined by a balance between receptor depletion and renewal at the cell surface. (A) In untreated cells, the internalisation and degradation of receptors is balanced by the synthesis and maturation of new receptors, and their renewal at the cell surface. Arrow size indicates relative rate. (B) In the presence of TGF-β, internalisation and degradation is faster than renewal, so receptors become depleted from the cell surface. (C) In the presence of activin, internalisation and degradation are matched by renewal, so no depletion is seen. (D) In the presence of BMP4, the balance is transiently tipped towards internalisation and degradation due to the upregulation of SMAD6/7, depleting receptors from the cell surface. In the presence of longer durations of BMP4, SMAD6 and SMAD7 are downregulated and internalisation and degradation are again matched by renewal. Receptors re-accumulate at the cell surface.

and thus will be mostly dissociated at the concentrations required for full bioactivity (Wang et al., 2016). Hence, active TGF-β is only generated when and where it is required, while activin and BMPs are essentially secreted as active ligands. We speculate that in the absence of any natural antagonists, the refractory behaviour exhibited by TGF-β after stimulation may be a defence against deregulated signalling, such as occurs in cancer and fibrosis (Akhurst and Hata, 2012).

Morphogen gradients have been shown to be gradients, not just of ligand concentration, but also of time (Kutejova et al., 2009). In the current paradigm, both the level of ligand and the duration of ligand exposure determines the fate of a cell in a gradient. For the activin, NODAL and BMP pathways, where signalling receptors accumulate over time while ligand is present, the levels of PSMAD are proportional to signal duration and ligand dose. In contrast, a cell in a TGF-β gradient would be unable to measure the duration of its exposure to ligand, as almost all signalling is initiated within the first few minutes. Moreover, a putative ligand antagonist would be unable to neutralise TGF-β, as most of the signalling occurs from internal compartments. Thus, TGF-β is regulated at the level of ligand production and release from the latency complex, and does not form signalling gradients.

BMP exhibits an oscillatory behaviour

We have demonstrated an oscillation in signalling downstream of BMP4 in multiple cell lines. This behaviour depends on the transient upregulation of SMAD6 and SMAD7, which are required for the transient depletion of BMPR2 from the cell surface, which in turn

correlates with the transient attenuation of signalling. The next step will be to investigate whether oscillations downstream of BMP signalling are observed in *in vivo* systems and what their function is. An attractive possibility is that they could be involved in periodically providing competence for cell fate decisions. It has been hypothesised that oscillatory behaviour of both BMP and Notch signalling is required for vascular patterning, in particular, in sprouting angiogenesis, to determine the selection of tip versus stalk cells (Beets et al., 2013; Moya et al., 2012). This idea was based on the scattered expression of *Id1*, *Id2* and *Id3* (prominent BMP target genes) in the mouse angiogenic epithelium, which was postulated to reflect a snapshot of non-synchronised oscillatory gene expression. It will be very interesting in the future to directly monitor BMP signalling live in this system to determine whether such oscillations occur.

MATERIALS AND METHODS
Cell lines and treatments
The human keratinocyte cell line HaCaT, the human breast cancer line MDA-MB-231, the mouse fibroblast cell line NIH-3T3 and the mouse teratoma cell line P19 were used throughout this study. HaCaT cells were obtained from the ATCC, MDA-MB-231 cells from the ECACC/HPA culture collection, NIH-3T3 cells were obtained from Richard Treisman (Francis Crick Institute, London, UK) and P19 cells were obtained from Grace Gill (Harvard Medical School, Boston, MA). All cell lines have been banked by the Francis Crick Institute Cell Services, and certified negative for mycoplasma. In addition, MDA-MB-231 and HaCaT cells were authenticated by short tandem repeat profiling, while NIH-3T3 and P19 cells had species confirmation at the Francis Crick Institute Cell Services. The identity of the cell lines was also authenticated by confirming that their responses to ligands, and their phenotypes were consistent with published history.

All cells were maintained in DMEM (Thermo Fisher Scientific), supplemented with 10% fetal calf serum (FCS). Ligands and reagents were used at the following concentrations: TGF-β (Peprotech), 2 ng/ml; BMP4 (Peprotech), 20 ng/ml; activin A (PeproTech), 20 ng/ml; noggin (PeproTech), 500 ng/ml; follistatin (Sigma), 500 ng/ml; LDN-193189 (a gift from Paul Yu, Brigham and Women's Hospital, Boston, MA), 1 μM; SB-431542 (Tocris), 10 μM; cycloheximide (Sigma), 20 μg/ml; actinomycin D (Sigma) 1 μg/ml. The TGF-β neutralising antibody, 1D11, and isotype-matched IgG1 monoclonal control antibody raised against *Shigella* toxin (13C4) were as described previously (Nam et al., 2008), and used at 30 μg/ml. All stimulations were performed in full serum. Where ligands or drugs were washed out, cells were washed three times with warm medium. Whole-cell extracts were prepared as previously described (Inman et al., 2002b). Where required, cell lysates were treated with PNGase F (New England Biosciences) at 500 U per 100 μg of protein.

Surface biotinylation and immunoblotting
Surface biotinylation assays were performed as previously described (Vizan et al., 2013). Immunoblotting was performed using standard techniques with the following antibodies, used at a dilution of 1:1000, except for those against BMPR2 and tubulin, which were used at 1:500 and 1:5000, respectively. Anti-PSMAD2 (Cell Signaling Technology, Cat. # 3108) (Ramachandran et al., 2018), anti-SMAD2/3 (BD Biosciences, Cat. # 610843) (Ramachandran et al., 2018), anti-PSMAD1/5 (Cat. # 13820) (Miller et al., 2018), anti-SMAD1 (Invitrogen, Cat. # 38-5400) (Ramachandran et al., 2018), anti-ACVR1B (Abcam, Cat. # Ab133478), anti-ACVR2B (Aviva Systems Biology, Cat. # ARP45041), anti-BMPR2 (BD Biosciences, Cat. # 612292), anti-TDGF1 (Cell Signaling Technology, Cat. # 2818) (Coda et al., 2017), anti-MCM6 (Santa Cruz, Cat. # sc-9843) (Miller et al., 2018) and anti-tubulin (Abcam, Cat. # Ab6160) (Ramachandran et al., 2018). The antibodies against ACVR1B, ACVR2B and BMPR2 were validated in this paper. Western blots were visualised on film or using an ImageQuant LAS 4000 mini (GE Healthcare) and quantified with ImageJ. For quantifications, densitometry measurements were normalised to loading controls and are shown relative to levels in cells stimulated with ligand for 1 h, except where indicated.

qPCR and siRNA knockdown
qPCR was performed as previously described (Gronroos et al., 2012). Primer sequences are given in Table S1. For siRNA experiments, cells were plated, and, 24 h later, transfected with 30 nM siRNA and 3 μl RNAiMax (Thermo Fisher Scientific), for NIH-3T3 cells and P19 cells, or 5 nM siRNA and 8 μl INTERFERin (PolyPlus), for MDA-MB-231 cells, and 200 μl Opti-MEM (Thermo Fisher Scientific) in fresh medium. In all cases, the effect of knockdown of a specific gene was compared with non-targeting siRNAs as a negative control. Volumes are given for a six-well plate. Experiments were performed 72 h after siRNA transfection. siRNAs were purchased from Dharmacon and sequences are given in Table S2. They were used as SMARTpools.

Statistical analysis
Student's *t*-tests were performed where appropriate using GraphPad Prism 7 software.

Mathematical modelling
The mathematical models of activin and BMP signalling are based on our previously published model of TGF-β signalling (Vizan et al., 2013), with the following key modifications.

Ligand binding to competent surface receptors is now treated as a reversible process. In the original TGF-β model, the dissociation rate of the ligand–receptor interaction was considered negligible compared to the activation of the receptor complex by the ligand, and ligand binding was treated as irreversible for simplicity. In the new model, this reaction is made reversible to allow modelling of different binding affinities of different ligands. An off-rate k'_{Toff} was thus introduced.

In addition, a negative-feedback mechanism mediated by I-SMADs was included to model the behaviour of cells in response to BMP4. I-SMADs were assumed to be synthesised in response to ligand, and to promote the degradation of signalling competent receptors, as well as the ligand-induced increase in degradation of active receptors.

I-SMADs are transcriptional targets of nuclear R-SMAD–SMAD4 complexes. Both I-SMAD RNA and protein were included to capture the time delay between ligand addition and I-SMAD expression. The two new equations for *I-SMAD* RNA and I-SMAD protein read:

$$\frac{dS_i^{RNA}}{dt} = k_{synbas}^{Ri} + k_{syn}^{Ri} S24_n^4 - k_{deg}^{Ri} S_i^{RNA}$$

$$\frac{dS_i}{dt} = k_{syn}^{Si} S_i^{RNA} - k_{deg}^{Si} S_i.$$

With these modifications, Eqns 2–5 from Vizan et al. (2013) now read (new terms indicated in bold):

$$\frac{1}{k_d}\frac{dR_{com}}{dt} = \alpha R - \frac{\boldsymbol{K_{Si} + S_i}}{\boldsymbol{K_{Si}}} R_{com}^I + \boldsymbol{k'_{Toff} R_T} - k'_T TGF\ R_{com}^S$$

$$\frac{1}{k_d}\frac{dR_T}{dt} = k'_T TGF\ R_{com}^s - \left(k'_{act} + \boldsymbol{k'_{Toff}} + D\ \frac{\boldsymbol{K_{Si} + S_i}}{\boldsymbol{K_{Si}}}\right) R_T$$

$$\frac{dR_{act}}{dt} = k'_{act} R_T - D\ \frac{\boldsymbol{K_{Si} + S_i}}{\boldsymbol{K_{Si}}} R_{act}$$

$$\frac{1}{k_d}\frac{dTGF}{dt} = \boldsymbol{k'_{Toff} R_T} - (k'_T R_{com}^S + k'_{cc})\ TGF.$$

The parameters used to model the behaviour of the I-SMADs are given in Table S3.

We have implemented these changes into a single model that can capture the dynamics of each ligand simply by changing the parameters in each case. Parameters that were changed to model each ligand are given in Table S4, with key parameter changes indicated in bold.

The key parameters changed are as follows: (1) The on-rate of ligand to receptor binding, k'_T, was chosen such that the dissociation constant of the ligand–receptor interaction, which is given by k'_{Toff}/k'_T, is very small for TGF-β (reflecting the high affinity of this ligand for its receptors), and is much larger for the other ligands. This is the only critical change necessary to alter the overall behaviour of the model in response to each ligand. (2) k'_{cc} is the constitutive clearance of the ligand from the medium. Assuming that BMP4 is cleared from the medium at the same speed as the other ligands

does not model the data well; it seems to be more persistent in the medium. (3) $k_{synT}^{\prime bas}$ is the basal ligand production, which is required for modelling activin dynamics in P19 cells, which secrete ligand in an autocrine fashion. (4) K_{SBI} is the dissociation constant of SB from the receptors. (5) Yes–No (Y/N) feedback is a toggle switch that allows us to switch on and off I-SMAD production in response to ligand.

In addition, alterations to the following parameters were necessary to accurately capture the experimental data were made. (1) k_d is the half-life of receptors in the absence of ligand. (2) D is the ligand-induced increase in degradation of active receptors. (3) $TSca$ scales the relative amounts of ligand to receptor.

The model was implemented in the freely available software packages COPASI (http://www.copasi.org) and XPP (http://www.math.pitt.edu/~bard/xpp/xpp.html). All simulations and parameter fitting were performed in COPASI (Hoops et al., 2006). The model has been deposited in the Biomodels database (Chelliah et al., 2015) and assigned the identifier MODEL1810160001.

References
Akhurst, R. J. and Hata, A. (2012). Targeting the TGFβ signalling pathway in disease. *Nat. Rev. Drug Discov.* **11**, 790-811. doi:10.1038/nrd3810

Attisano, L., Wrana, J. L., Cheifetz, S. and Massague, J. (1992). Novel activin receptors: distinct genes and alternative mRNA splicing generate a repertoire of serine/threonine kinase receptors. *Cell* **68**, 97-108. doi:10.1016/0092-8674(92)90209-U

Beets, K., Huylebroeck, D., Moya, I. M., Umans, L. and Zwijsen, A. (2013). Robustness in angiogenesis: notch and BMP shaping waves. *Trends Genet.* **29**, 140-149. doi:10.1016/j.tig.2012.11.008

Brazil, D. P., Church, R. H., Surae, S., Godson, C. and Martin, F. (2015). BMP signalling: agony and antagony in the family. *Trends Cell Biol.* **25**, 249-264. doi:10.1016/j.tcb.2014.12.004

Chelliah, V., Juty, N., Ajmera, I., Ali, R., Dumousseau, M., Glont, M., Hucka, M., Jalowicki, G., Keating, S., Knight-Schrijver, V. et al. (2015). BioModels: ten-year anniversary. *Nucleic Acids Res.* **43**, D542-D548. doi:10.1093/nar/gku1181

Clarke, D. C. and Liu, X. (2008). Decoding the quantitative nature of TGF-β/Smad signaling. *Trends Cell Biol.* **18**, 430-442. doi:10.1016/j.tcb.2008.06.006

Coda, D. M., Gaarenstroom, T., East, P., Patel, H., Miller, D. S. J., Lobley, A., Matthews, N., Stewart, A. and Hill, C. S. (2017). Distinct modes of SMAD2 chromatin binding and remodeling shape the transcriptional response to NODAL/Activin signaling. *eLife* **6**, e22474. doi:10.7554/eLife.22474

Cuny, G. D., Yu, P. B., Laha, J. K., Xing, X., Liu, J.-F., Lai, C. S., Deng, D. Y., Sachidanandan, C., Bloch, K. D. and Peterson, R. T. (2008). Structure-activity relationship study of bone morphogenetic protein (BMP) signaling inhibitors. *Bioorg. Med. Chem. Lett.* **18**, 4388-4392. doi:10.1016/j.bmcl.2008.06.052

Daly, A. C., Randall, R. A. and Hill, C. S. (2008). Transforming growth factor β-induced Smad1/5 phosphorylation in epithelial cells is mediated by novel receptor complexes and is essential for anchorage-independent growth. *Mol. Cell. Biol.* **28**, 6889-6902. doi:10.1128/MCB.01192-08

De Crescenzo, G., Pham, P. L., Durocher, Y. and O'Connor-McCourt, M. D. (2003). Transforming growth factor-β (TGF-β) binding to the extracellular domain of the type II TGF-β receptor: receptor capture on a biosensor surface using a new coiled-coil capture system demonstrates that avidity contributes significantly to high affinity binding. *J. Mol. Biol.* **328**, 1173-1183. doi:10.1016/S0022-2836(03)00360-7

Di Guglielmo, G. M., Le Roy, C., Goodfellow, A. F. and Wrana, J. L. (2003). Distinct endocytic pathways regulate TGF-β receptor signalling and turnover. *Nat. Cell Biol.* **5**, 410-421. doi:10.1038/ncb975

Dudas, M., Kim, J., Li, W.-Y., Nagy, A., Larsson, J., Karlsson, S., Chai, Y. and Kaartinen, V. (2006). Epithelial and ectomesenchymal role of the type I TGF-β receptor ALK5 during facial morphogenesis and palatal fusion. *Dev. Biol.* **296**, 298-314. doi:10.1016/j.ydbio.2006.05.030

Ebisawa, T., Fukuchi, M., Murakami, G., Chiba, T., Tanaka, K., Imamura, T. and Miyazono, K. (2001). Smurf1 interacts with transforming growth factor β I receptor through Smad7 and induces receptor degradation. *J. Biol. Chem.* **276**, 12477-12480. doi:10.1074/jbc.C100008200

Goto, K., Kamiya, Y., Imamura, T., Miyazono, K. and Miyazawa, K. (2007). Selective inhibitory effects of Smad6 on bone morphogenetic protein type I receptors. *J. Biol. Chem.* **282**, 20603-20611. doi:10.1074/jbc.M702100200

Gronroos, E., Kingston, I. J., Ramachandran, A., Randall, R. A., Vizan, P. and Hill, C. S. (2012). Transforming growth factor β inhibits bone morphogenetic protein-induced transcription through novel phosphorylated Smad1/5-Smad3 complexes. *Mol. Cell. Biol.* **32**, 2904-2916. doi:10.1128/MCB.00231-12

Groppe, J., Hinck, C. S., Samavarchi-Tehrani, P., Zubieta, C., Schuermann, J. P., Taylor, A. B., Schwarz, P. M., Wrana, J. L. and Hinck, A. P. (2008). Cooperative assembly of TGF-β superfamily signaling complexes is mediated by two disparate mechanisms and distinct modes of receptor binding. *Mol. Cell* **29**, 157-168. doi:10.1016/j.molcel.2007.11.039

Gurdon, J. B., Harger, P., Mitchell, A. and Lemaire, P. (1994). Activin signalling and response to a morphogen gradient. *Nature* **371**, 487-492. doi:10.1038/371487a0

Hata, A., Lagna, G., Massague, J. and Hemmati-Brivanlou, A. (1998). Smad6 inhibits BMP/Smad1 signaling by specifically competing with the Smad4 tumor suppressor. *Genes Dev.* **12**, 186-197. doi:10.1101/gad.12.2.186

Hatsell, S. J., Idone, V., Wolken, D. M., Huang, L., Kim, H. J., Wang, L., Wen, X., Nannuru, K. C., Jimenez, J., Xie, L. et al. (2015). ACVR1R206H receptor mutation causes fibrodysplasia ossificans progressiva by imparting responsiveness to activin A. *Sci. Transl. Med.* **7**, 303ra137. doi:10.1126/scitranslmed.aac4358

Hayashi, H., Abdollah, S., Qiu, Y., Cai, J., Xu, Y.-Y., Grinnell, B. W., Richardson, M. A., Topper, J. N., Gimbrone, M. A., Jr, Wrana, J. L. et al. (1997). The MAD-related protein Smad7 associates with the TGFβ receptor and functions as an antagonist of TGFβ signaling. *Cell* **89**, 1165-1173. doi:10.1016/S0092-8674(00)80303-7

He, K., Yan, X., Li, N., Dang, S., Xu, L., Zhao, B., Li, Z., Lv, Z., Fang, X., Zhang, Y. et al. (2015). Internalization of the TGF-β type I receptor into caveolin-1 and EEA1 double-positive early endosomes. *Cell Res.* **25**, 738-752. doi:10.1038/cr.2015.60

Hedger, M. P. and de Kretser, D. M. (2013). The activins and their binding protein, follistatin-Diagnostic and therapeutic targets in inflammatory disease and fibrosis. *Cytokine Growth Factor. Rev.* **24**, 285-295. doi:10.1016/j.cytogfr.2013.03.003

Heldin, C.-H. and Moustakas, A. (2016). Signaling receptors for TGF-β family members. *Cold Spring Harb. Perspect. Biol.* **8**, a022053. doi:10.1101/cshperspect.a022053

Hill, C. S. (2018). Spatial and temporal control of NODAL signaling. *Curr. Opin. Cell Biol.* **51**, 50-57. doi:10.1016/j.ceb.2017.10.005

Hinck, A. P. (2012). Structural studies of the TGF-βs and their receptors - insights into evolution of the TGF-β superfamily. *FEBS Lett.* **586**, 1860-1870. doi:10.1016/j.febslet.2012.05.028

Hoops, S., Sahle, S., Gauges, R., Lee, C., Pahle, J., Simus, N., Singhal, M., Xu, L., Mendes, P. and Kummer, U. (2006). COPASI–a COmplex PAthway SImulator. *Bioinformatics* **22**, 3067-3074. doi:10.1093/bioinformatics/btl485

Imamura, T., Takase, M., Nishihara, A., Oeda, E., Hanai, J.-I., Kawabata, M. and Miyazono, K. (1997). Smad6 inhibits signalling by the TGF-β superfamily. *Nature* **389**, 622-626. doi:10.1038/39355

Inman, G. J., Nicolas, F. J., Callahan, J. F., Harling, J. D., Gaster, L. M., Reith, A. D., Laping, N. J. and Hill, C. S. (2002a). SB-431542 is a potent and specific inhibitor of transforming growth factor-β superfamily type I activin receptor-like kinase (ALK) receptors ALK4, ALK5, and ALK7. *Mol. Pharmacol.* **62**, 65-74. doi:10.1124/mol.62.1.65

Inman, G. J., Nicolás, F. J. and Hill, C. S. (2002b). Nucleocytoplasmic shuttling of Smads 2, 3, and 4 permits sensing of TGF-β receptor activity. *Mol. Cell* **10**, 283-294. doi:10.1016/S1097-2765(02)00585-3

Itoh, F., Divecha, N., Brocks, L., Oomen, L., Janssen, H., Calafat, J., Itoh, S. and ten Dijke, P. (2002). The FYVE domain in Smad anchor for receptor activation (SARA) is sufficient for localization of SARA in early endosomes and regulates TGF-β/Smad signalling. *Genes Cells* **7**, 321-331. doi:10.1046/j.1365-2443.2002.00519.x

Kavsak, P., Rasmussen, R. K., Causing, C. G., Bonni, S., Zhu, H., Thomsen, G. H. and Wrana, J. L. (2000). Smad7 binds to Smurf2 to form an E3 ubiquitin ligase that targets the TGFβ receptor for degradation. *Mol. Cell* **6**, 1365-1375. doi:10.1016/S1097-2765(00)00134-9

Kutejova, E., Briscoe, J. and Kicheva, A. (2009). Temporal dynamics of patterning by morphogen gradients. *Curr. Opin. Genet. Dev.* **19**, 315-322. doi:10.1016/j.gde. 2009.05.004

Langdon, Y. G. and Mullins, M. C. (2011). Maternal and zygotic control of zebrafish dorsoventral axial patterning. *Annu. Rev. Genet.* **45**, 357-377. doi:10.1146/ annurev-genet-110410-132517

Le Roy, C. and Wrana, J. L. (2005). Clathrin- and non-clathrin-mediated endocytic regulation of cell signalling. *Nat. Rev. Mol. Cell Biol.* **6**, 112-126. doi:10.1038/ nrm1571

Lin, X., Liang, Y.-Y., Sun, B., Liang, M., Shi, Y., Brunicardi, F. C., Shi, Y. and Feng, X.-H. (2003). Smad6 recruits transcription corepressor CtBP to repress bone morphogenetic protein-induced transcription. *Mol. Cell. Biol.* **23**, 9081-9093. doi:10.1128/MCB.23.24.9081-9093.2003

Luyten, F. P., Chen, P., Paralkar, V. and Reddi, A. H. (1994). Recombinant bone morphogenetic protein-4, transforming growth factor-β1, and activin A enhance the cartilage phenotype of articular chondrocytes in vitro. *Exp. Cell Res.* **210**, 224-229. doi:10.1006/excr.1994.1033

Massagué, J. (1990). The transforming growth factor-β family. *Annu. Rev. Cell Biol.* **6**, 597-641. doi:10.1146/annurev.cb.06.110190.003121

Massagué, J. (2008). TGFβ in cancer. *Cell* **134**, 215-230. doi:10.1016/j.cell.2008. 07.001

Mercado-Pimentel, M. E. and Runyan, R. B. (2007). Multiple transforming growth factor-β isoforms and receptors function during epithelial-mesenchymal cell transformation in the embryonic heart. *Cells Tissues Organs* **185**, 146-156. doi:10.1159/000101315

Mi, L. Z., Brown, C. T., Gao, Y., Tian, Y., Le, V. Q., Walz, T. and Springer, T. A. (2015). Structure of bone morphogenetic protein 9 procomplex. *Proc. Natl. Acad. Sci. USA* **112**, 3710-3715. doi:10.1073/pnas.1501303112

Miller, D. S. J. and Hill, C. S. (2016). TGF-β superfamily signalling. In *Encyclopedia of Cell Biology*, Vol. 3 (ed. R. A. Bradshaw and P. D. Stahl), pp. 37-50. Elsevier.

Miller, D. S. J., Bloxham, R. D., Jiang, M., Gori, I., Saunders, R. E., Das, D., Chakravarty, P., Howell, M. and Hill, C. S. (2018). The dynamics of TGF-β signaling are dictated by receptor trafficking via the ESCRT machinery. *Cell Rep.* **25**, 1841-1855.e1845. doi:10.1016/j.celrep.2018.10.056

Mitchell, H., Choudhury, A., Pagano, R. E. and Leof, E. B. (2004). Ligand-dependent and -independent transforming growth factor-β receptor recycling regulated by clathrin-mediated endocytosis and Rab11. *Mol. Biol. Cell* **15**, 4166-4178. doi:10.1091/mbc.e04-03-0245

Moses, H. L., Roberts, A. B. and Derynck, R. (2016). The discovery and early days of TGF-β: a historical perspective. *Cold Spring Harb. Perspect. Biol.* **8**, a021865. doi:10.1101/cshperspect.a021865

Moya, I. M., Umans, L., Maas, E., Pereira, P. N. G., Beets, K., Francis, A., Sents, W., Robertson, E. J., Mummery, C. L., Huylebroeck, D. et al. (2012). Stalk cell phenotype depends on integration of Notch and Smad1/5 signaling cascades. *Dev. Cell* **22**, 501-514. doi:10.1016/j.devcel.2012.01.007

Nakamura, T., Takio, K., Eto, Y., Shibai, H., Titani, K. and Sugino, H. (1990). Activin-binding protein from rat ovary is follistatin. *Science* **247**, 836-838. doi:10. 1126/science.2106159

Nakao, A., Afrakhte, M., Morn, A., Nakayama, T., Christian, J. L., Heuchel, R., Itoh, S., Kawabata, M., Heldin, N.-E., Heldin, C.-H. et al. (1997). Identification of Smad7, a TGFβ-inducible antagonist of TGF-β signalling. *Nature* **389**, 631-635. doi:10.1038/39369

Nam, J.-S., Terabe, M., Mamura, M., Kang, M.-J., Chae, H., Stuelten, C., Kohn, E., Tang, B., Sabzevari, H., Anver, M. R. et al. (2008). An anti-transforming growth factor β antibody suppresses metastasis via cooperative effects on multiple cell compartments. *Cancer Res.* **68**, 3835-3843. doi:10.1158/0008-5472.CAN-08-0215

Pagliuca, F. W., Millman, J. R., Gürtler, M., Segel, M., Van Dervort, A., Ryu, J. H., Peterson, Q. P., Greiner, D. and Melton, D. A. (2014). Generation of functional human pancreatic β cells in vitro. *Cell* **159**, 428-439. doi:10.1016/j.cell. 2014.09.040

Pickup, M. W., Owens, P. and Moses, H. L. (2017). TGF-β, bone morphogenetic protein, and activin signaling and the tumor microenvironment. *Cold Spring Harb. Perspect. Biol.* **9**, a022285. doi:10.1101/cshperspect.a022285

Pomreinke, A. P., Soh, G. H., Rogers, K. W., Bergmann, J. K., Blässle, A. J. and Müller, P. (2017). Dynamics of BMP signaling and distribution during zebrafish dorsal-ventral patterning. *eLife* **6**, e25861. doi:10.7554/eLife.25861

Ramachandran, A., Vizán, P., Das, D., Chakravarty, P., Vogt, J., Rogers, K. W., Müller, P., Hinck, A. P., Sapkota, G. P. and Hill, C. S. (2018). TGF-β uses a novel mode of receptor activation to phosphorylate SMAD1/5 and induce epithelial-to-mesenchymal transition. *eLife* **7**, e31756. doi:10.7554/eLife.31756

Ramel, M.-C. and Hill, C. S. (2013). The ventral to dorsal BMP activity gradient in the early zebrafish embryo is determined by graded expression of BMP ligands. *Dev. Biol.* **378**, 170-182. doi:10.1016/j.ydbio.2013.03.003

Schier, A. F. (2009). Nodal morphogens. *Cold Spring Harb. Perspect. Biol.* **1**, a003459. doi:10.1101/cshperspect.a003459

Schier, A. F. and Talbot, W. S. (2005). Molecular genetics of axis formation in zebrafish. *Annu. Rev. Genet.* **39**, 561-613. doi:10.1146/annurev.genet.37. 110801.143752

Schmierer, B. and Hill, C. S. (2007). TGFβ-SMAD signal transduction: molecular specificity and functional flexibility. *Nat. Rev. Mol. Cell Biol.* **8**, 970-982. doi:10. 1038/nrm2297

Schmierer, B., Tournier, A. L., Bates, P. A. and Hill, C. S. (2008). Mathematical modeling identifies Smad nucleocytoplasmic shuttling as a dynamic signal-interpreting system. *Proc. Natl. Acad. Sci. USA* **105**, 6608-6613. doi:10.1073/ pnas.0710134105

Takase, M., Imamura, T., Sampath, T. K., Takeda, K., Ichijo, H., Miyazono, K. and Kawabata, M. (1998). Induction of Smad6 mRNA by bone morphogenetic proteins. *Biochem. Biophys. Res. Commun.* **244**, 26-29. doi:10.1006/bbrc.1998. 8200

ten Dijke, P. and Arthur, H. M. (2007). Extracellular control of TGFβ signalling in vascular development and disease. *Nat. Rev. Mol. Cell Biol.* **8**, 857-869. doi:10. 1038/nrm2262

Tsuchida, K., Nakatani, M., Hitachi, K., Uezumi, A., Sunada, Y., Ageta, H. and Inokuchi, K. (2009). Activin signaling as an emerging target for therapeutic interventions. *Cell Commun. Signal.* **7**, 15. doi:10.1186/1478-811X-7-15

van Boxtel, A. L., Chesebro, J. E., Heliot, C., Ramel, M.-C., Stone, R. K. and Hill, C. S. (2015). A temporal window for signal activation dictates the dimensions of a nodal signaling domain. *Dev. Cell* **35**, 175-185. doi:10.1016/j. devcel.2015.09.014

Vizan, P., Miller, D. S. J., Gori, I., Das, D., Schmierer, B. and Hill, C. S. (2013). Controlling long-term signaling: receptor dynamics determine attenuation and refractory behavior of the TGF-β pathway. *Sci. Signal.* **6**, ra106. doi:10.1126/ scisignal.2004416

Wang, X., Fischer, G. and Hyvönen, M. (2016). Structure and activation of pro-activin A. *Nat. Commun.* **7**, 12052. doi:10.1038/ncomms12052

Wharton, K. A., Ray, R. P. and Gelbart, W. M. (1993). An activity gradient of decapentaplegic is necessary for the specification of dorsal pattern elements in the Drosophila embryo. *Development* **117**, 807-822.

Yakymovych, I., Yakymovych, M. and Heldin, C.-H. (2018). Intracellular trafficking of transforming growth factor β receptors. *Acta Biochim. Biophys. Sin. (Shanghai)* **50**, 3-11. doi:10.1093/abbs/gmx119

Zimmerman, L. B., De Jesús-Escobar, J. M. and Harland, R. M. (1996). The Spemann organizer signal noggin binds and inactivates bone morphogenetic protein 4. *Cell* **86**, 599-606. doi:10.1016/S0092-8674(00)80133-6

Zinski, J., Bu, Y., Wang, X., Dou, W., Umulis, D. and Mullins, M. C. (2017). Systems biology derived source-sink mechanism of BMP gradient formation. *eLife* **6**, e22199. doi:10.7554/eLife.22199